

Supplement of Atmos. Chem. Phys., 16, 6913–6929, 2016
<http://www.atmos-chem-phys.net/16/6913/2016/>
doi:10.5194/acp-16-6913-2016-supplement
© Author(s) 2016. CC Attribution 3.0 License.



Atmospheric
Chemistry
and Physics
Open Access
EGU

Supplement of

Diurnal variation of tropospheric relative humidity in tropical regions

Isaac Moradi et al.

Correspondence to: Isaac Moradi (isaac.moradi@nasa.gov)

The copyright of individual parts of the supplement might differ from the CC-BY 3.0 licence.

1 RH Spatial Distribution

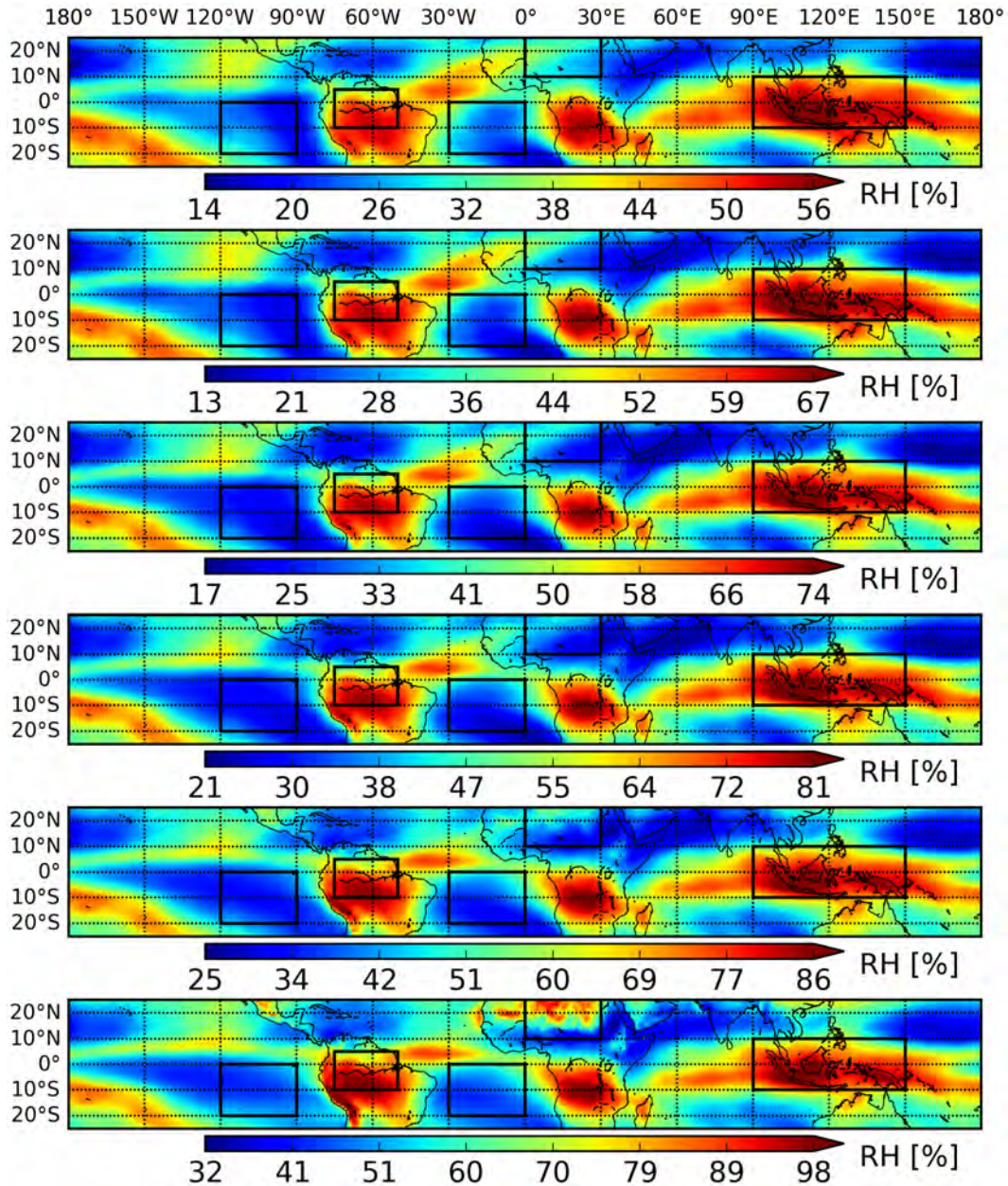


Figure 1. Spatial distribution of layer-averaged RH_l derived using SAPHIR data for December and January. Depicts from top to bottom are for SAPHIR channels 1-6, respectively.

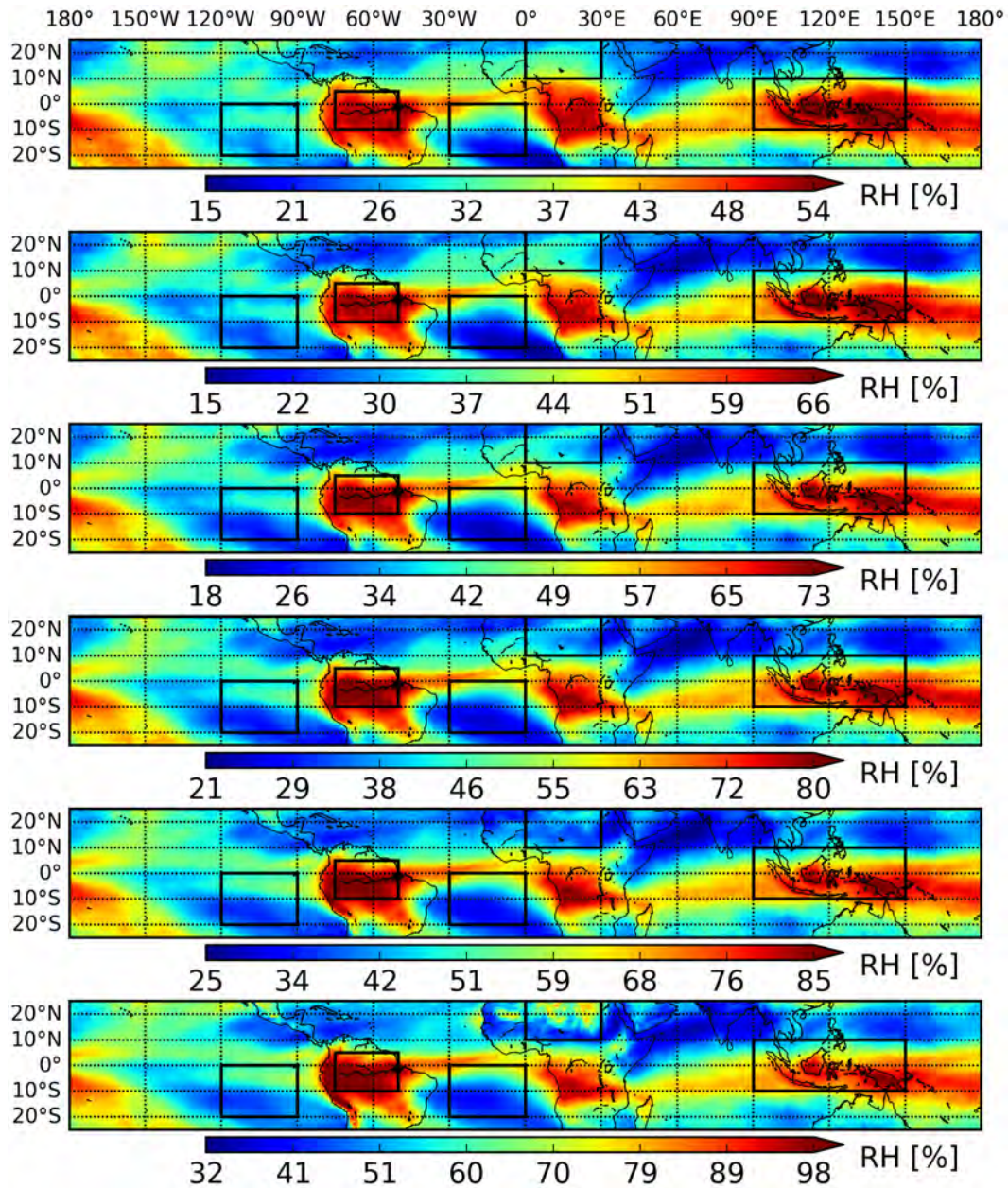


Figure 2. Spatial distribution of layer-averaged RH_l derived using SAPHIR data for the Month March. Depicts from top to bottom are for SAPHIR channels 1-6, respectively.

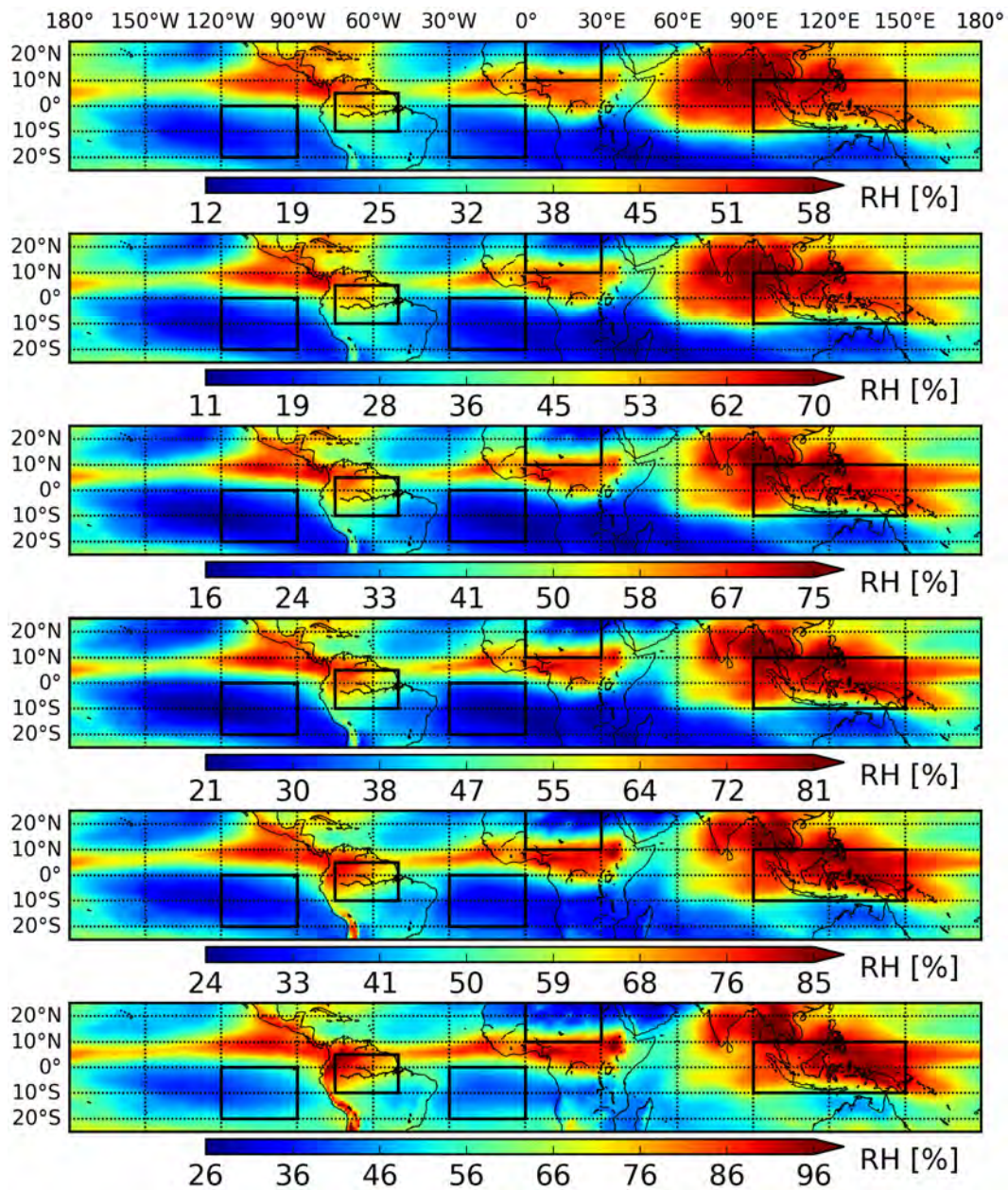


Figure 3. Spatial distribution of layer-averaged RH_I derived using SAPHIR data for June and July. Depicts from top to bottom are for SAPHIR channels 1-6, respectively.

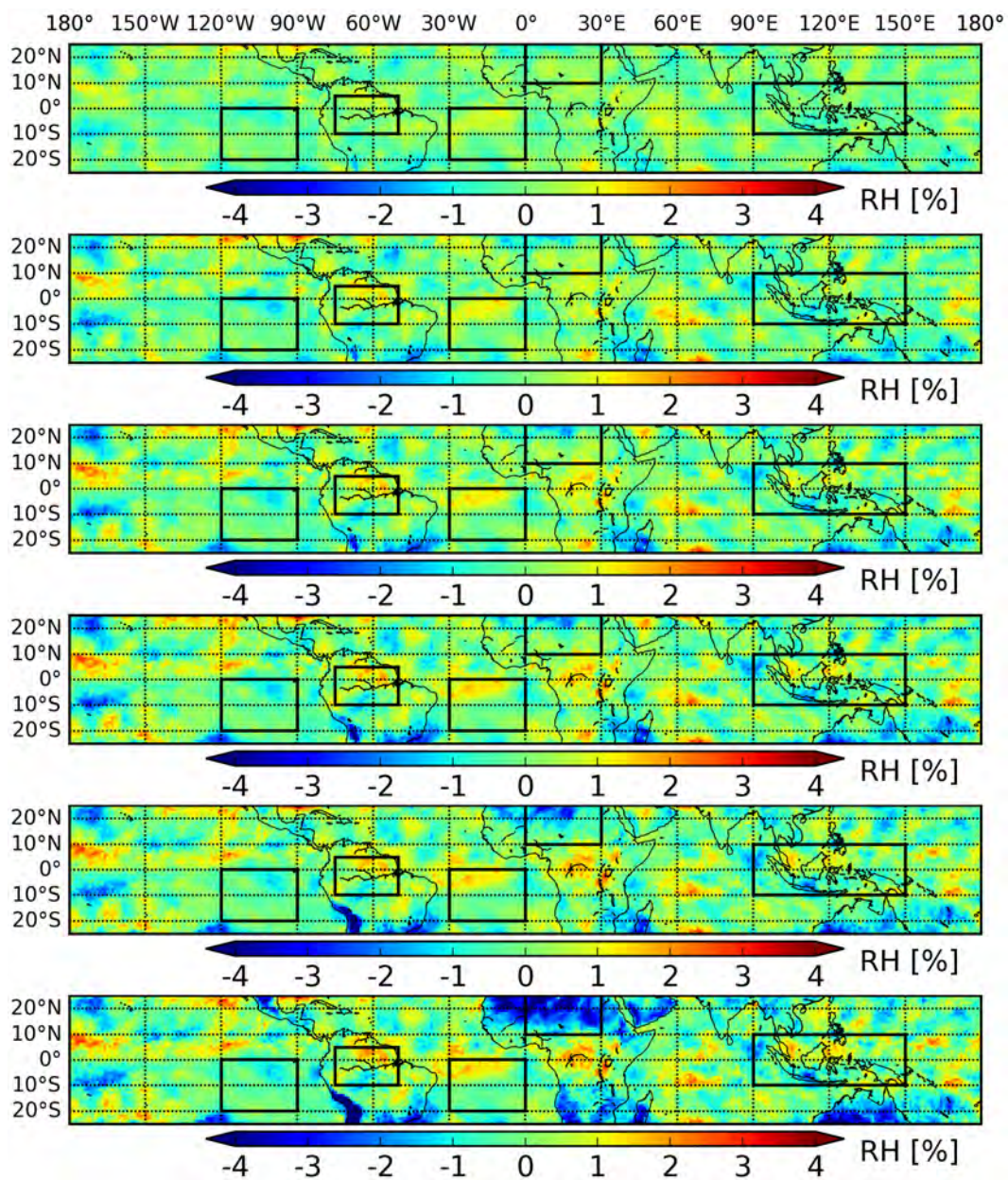


Figure 4. Mean difference of daily average of RH_L calculated using only data from 01:30/13:30 local time and the daily average calculated using all hourly data. Plots from top to bottom are for SAPHIR channels 1-6, respectively.

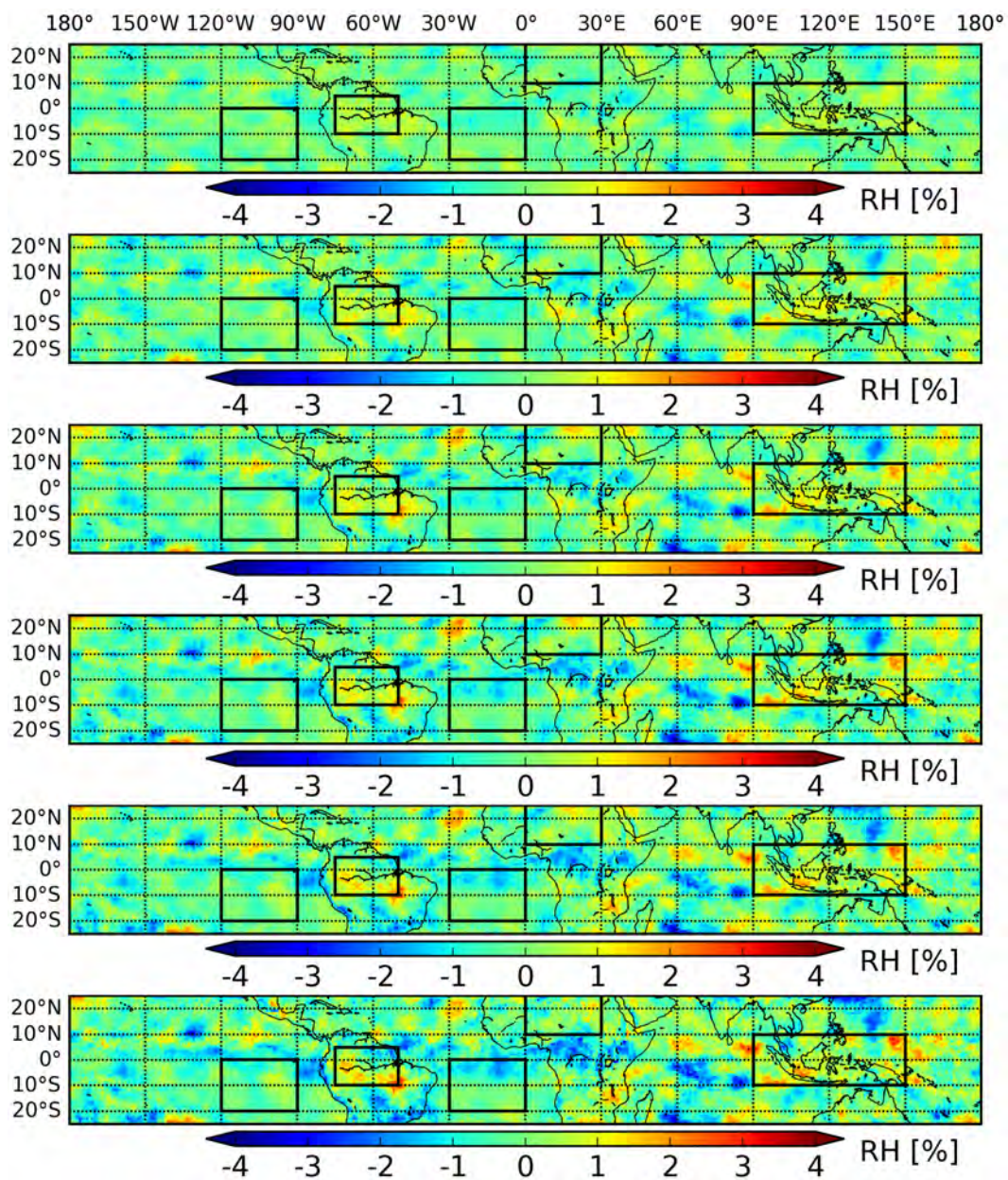


Figure 5. Mean difference of daily average of RH_L calculated using only data from 09:30/21:30 local time and the daily average calculated using all hourly data. Plots from top to bottom are for SAPHIR channels 1-6, respectively.

2 RH Peak and Amplitudes (Measurements)

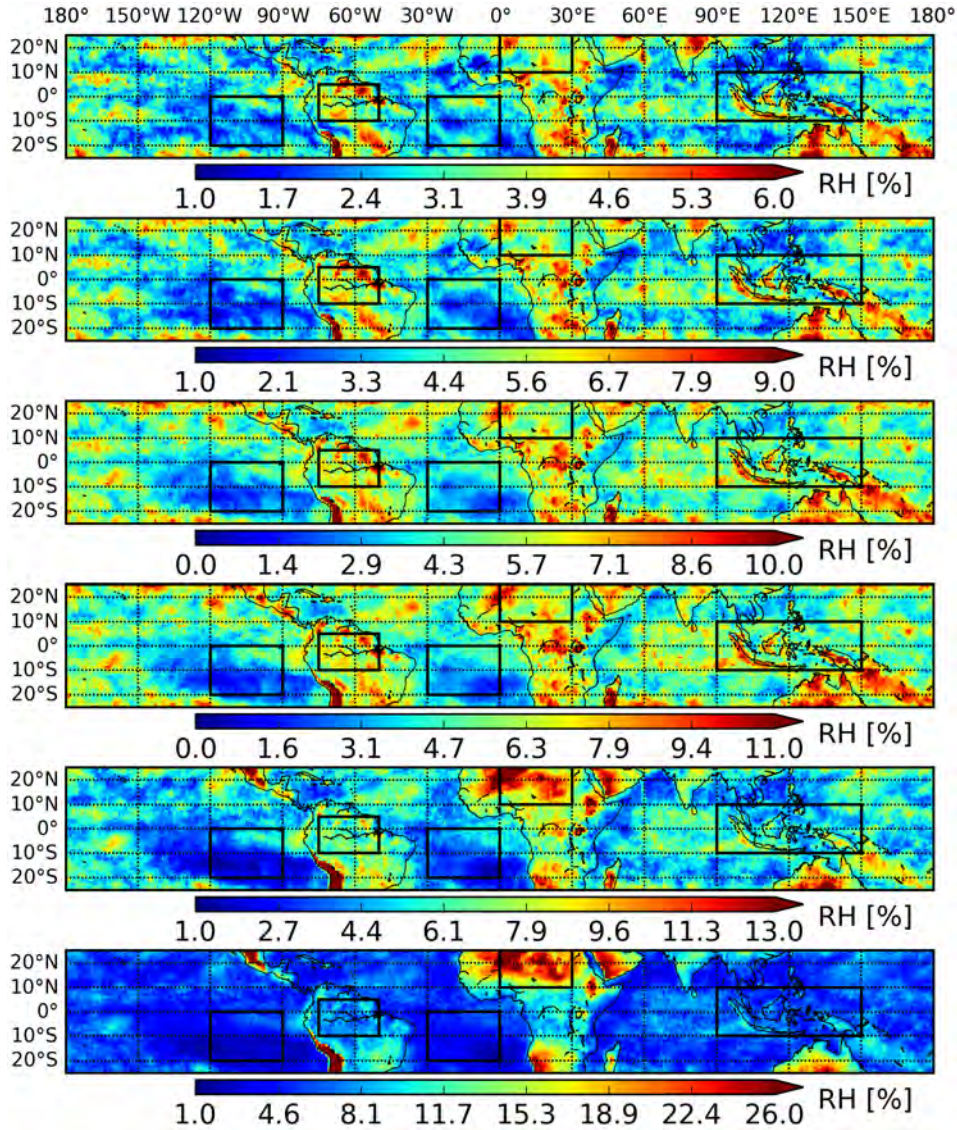


Figure 6. Spatial distribution of diurnal amplitude of tropospheric humidity over liquid (based on measurements). Plots from top to bottom are for SAPHIR channels 1-6, respectively.

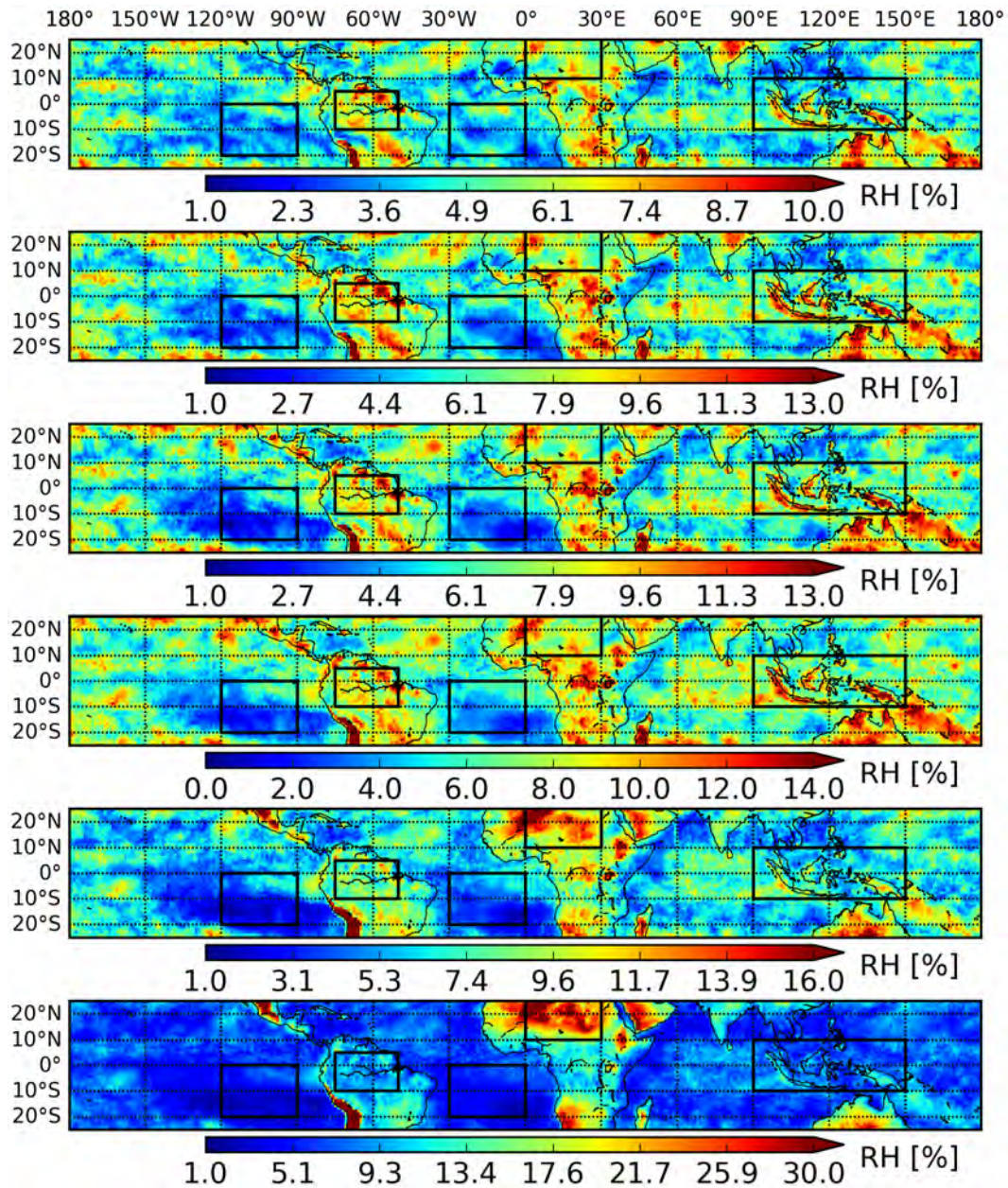


Figure 7. Spatial distribution of diurnal amplitude of tropospheric humidity over ice (based on measurements). Plots from top to bottom are for SAPHIR channels 1-6, respectively.

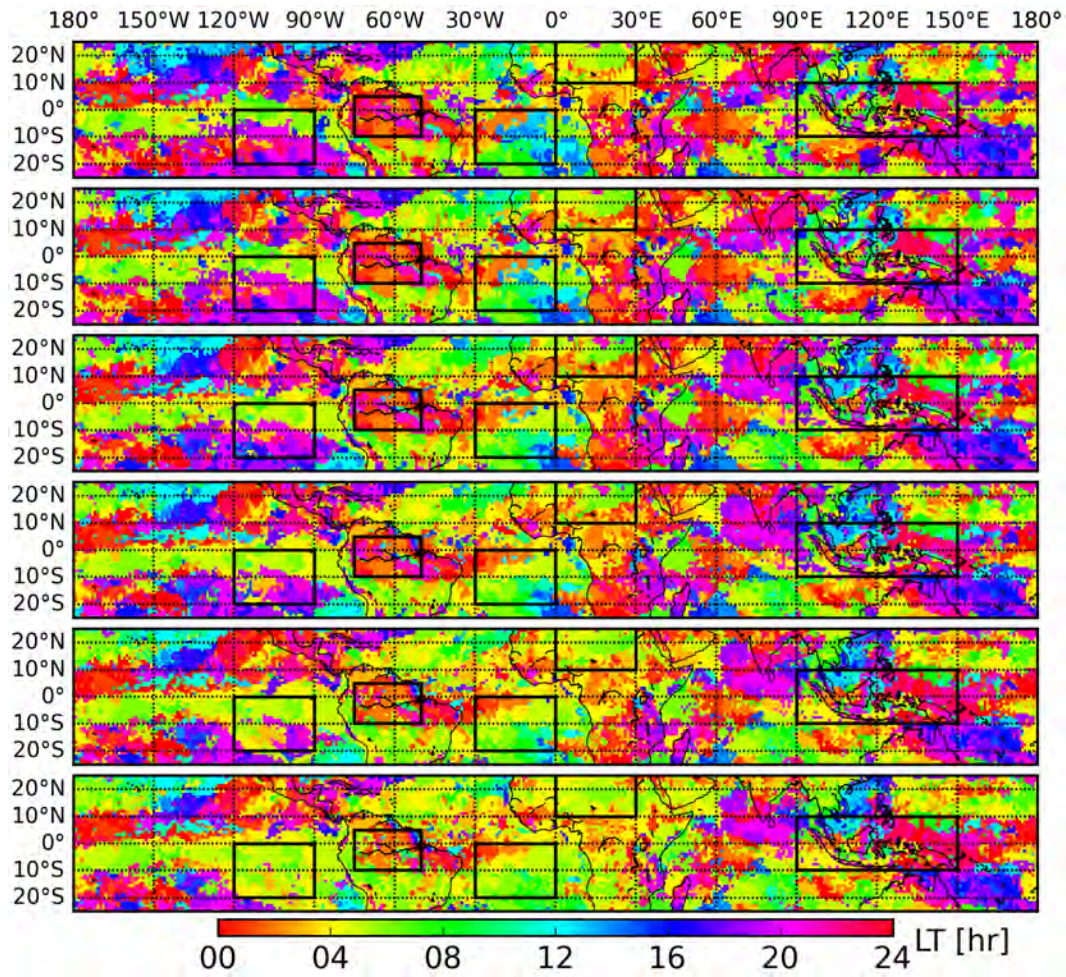


Figure 8. Diurnal peak time (based on measurements with respect to liquid) for upper to lower tropospheric channels (SAPHIR channels 1-6 from top to bottom) in local time.

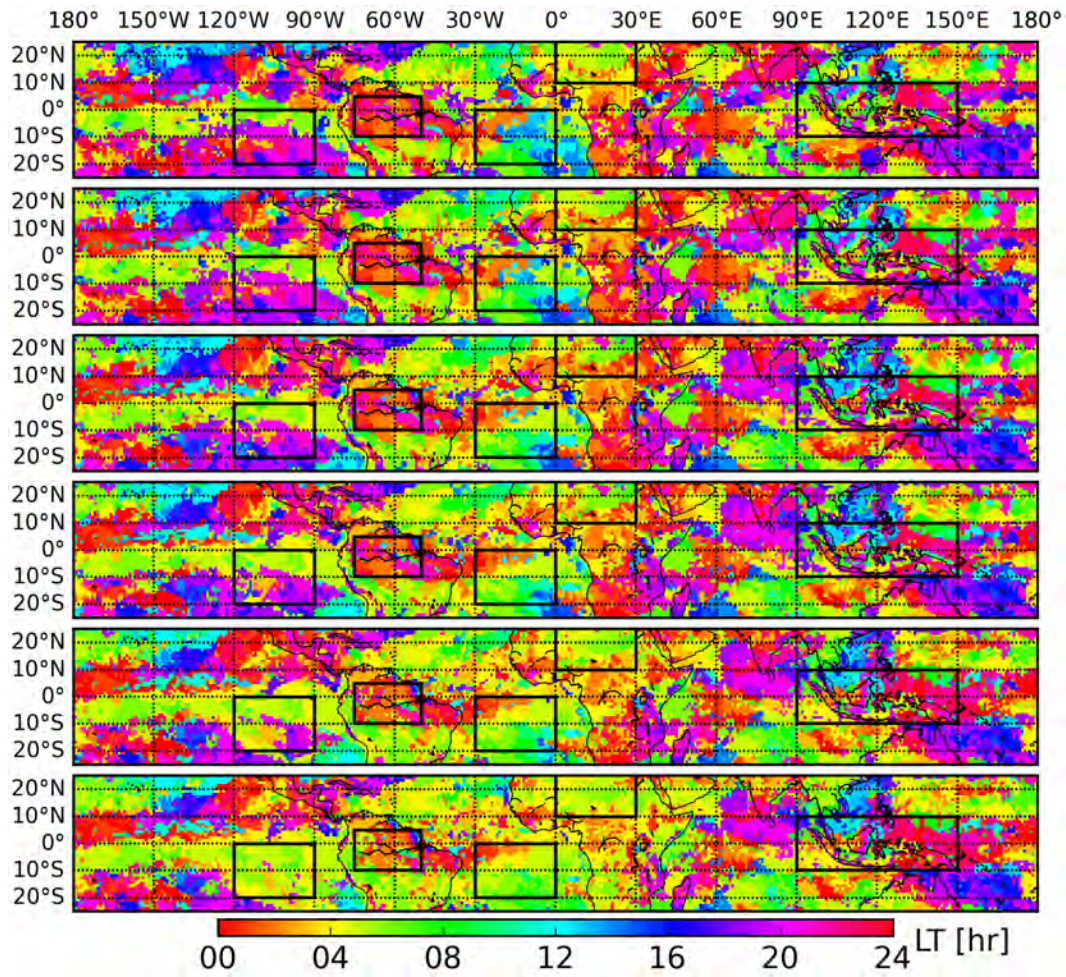


Figure 9. Diurnal peak time (based on measurements with respect to ice) for upper to lower tropospheric channels (SAPHIR channels 1-6 from top to bottom) in local time.

3 RH Peak and Amplitudes Derived From Fourier Series

5

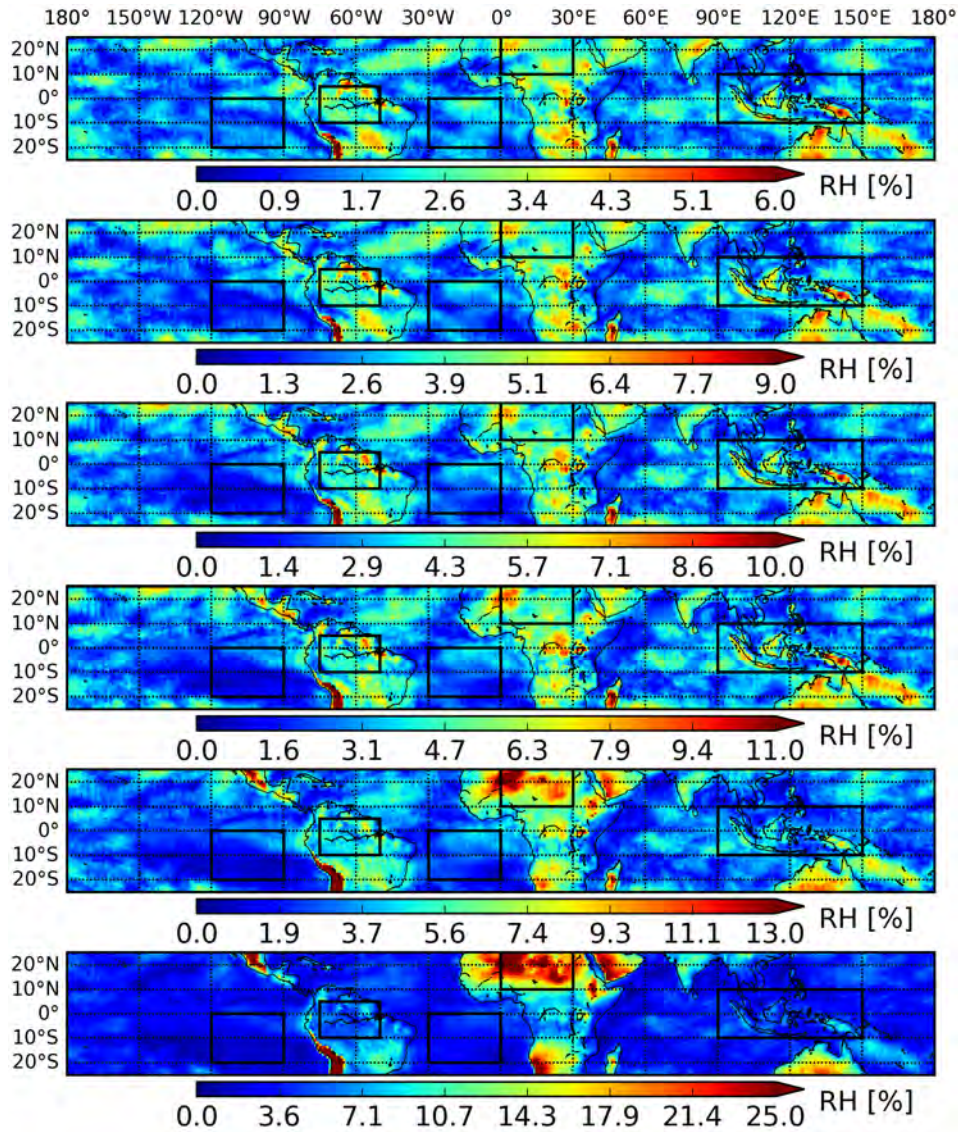


Figure 10. Spatial distribution of diurnal amplitude of tropospheric humidity over liquid (based on the Fourier series fit). Plots from top to bottom are for SAPHIR channels 1-6, respectively.

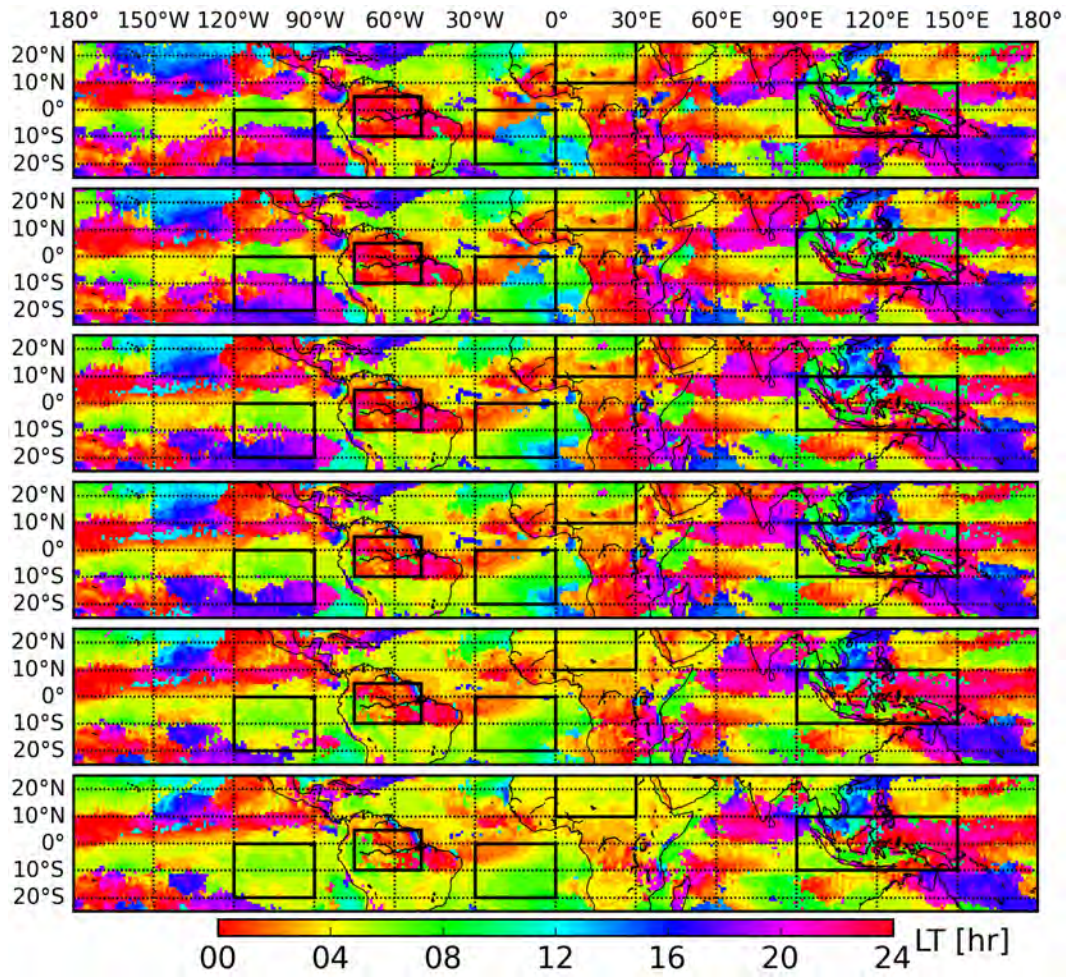


Figure 11. Diurnal peak time (with respect to liquid and based on Fourier series fit) in local time. Plots from top to bottom are for SAPHIR channels 1-6, respectively.

4 Fourier Series

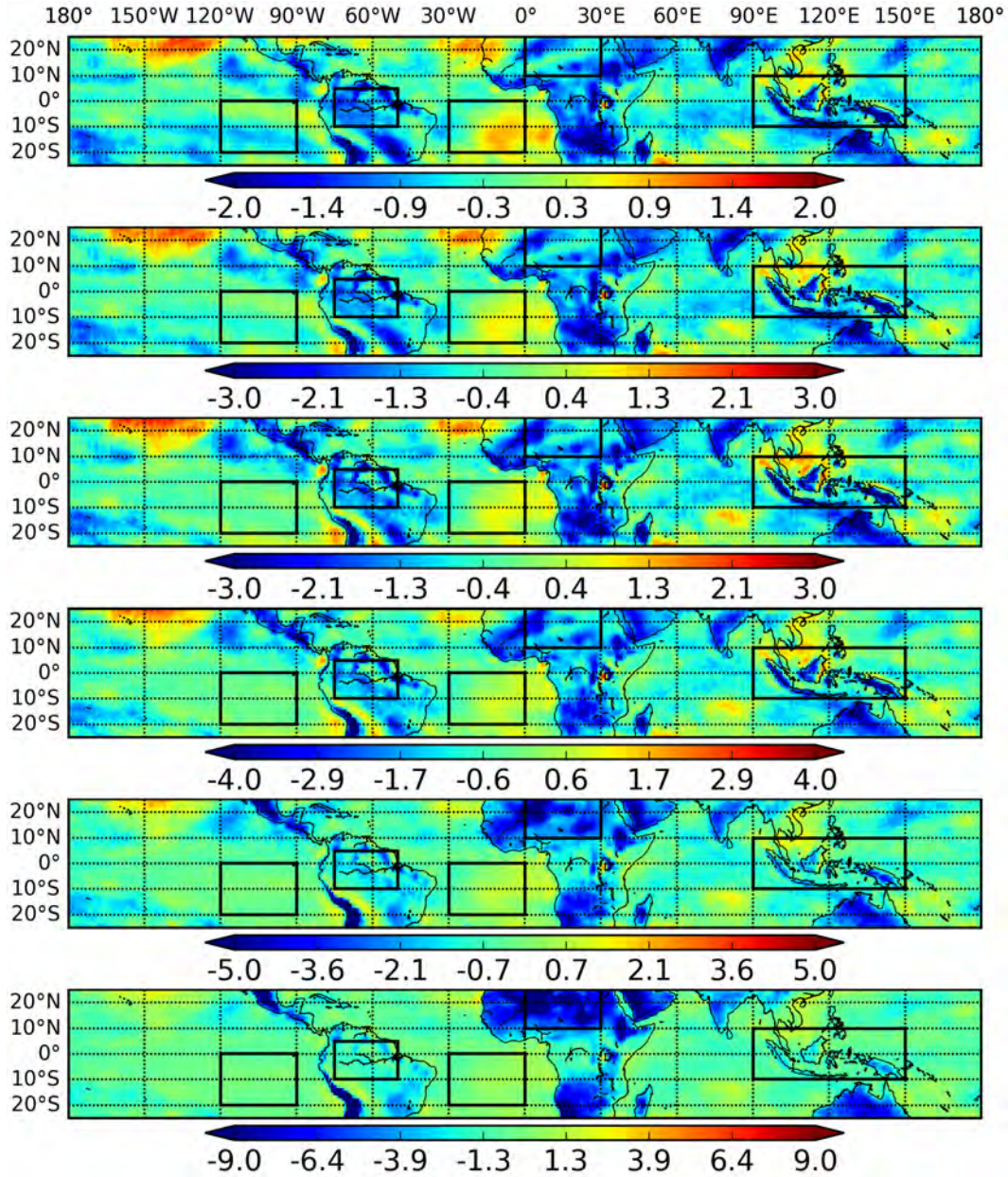


Figure 12. The coefficient a_1 (with respect to liquid) for the Fourier series fit. Plots from top to bottom are for SAPHIR channels 1-6, respectively.

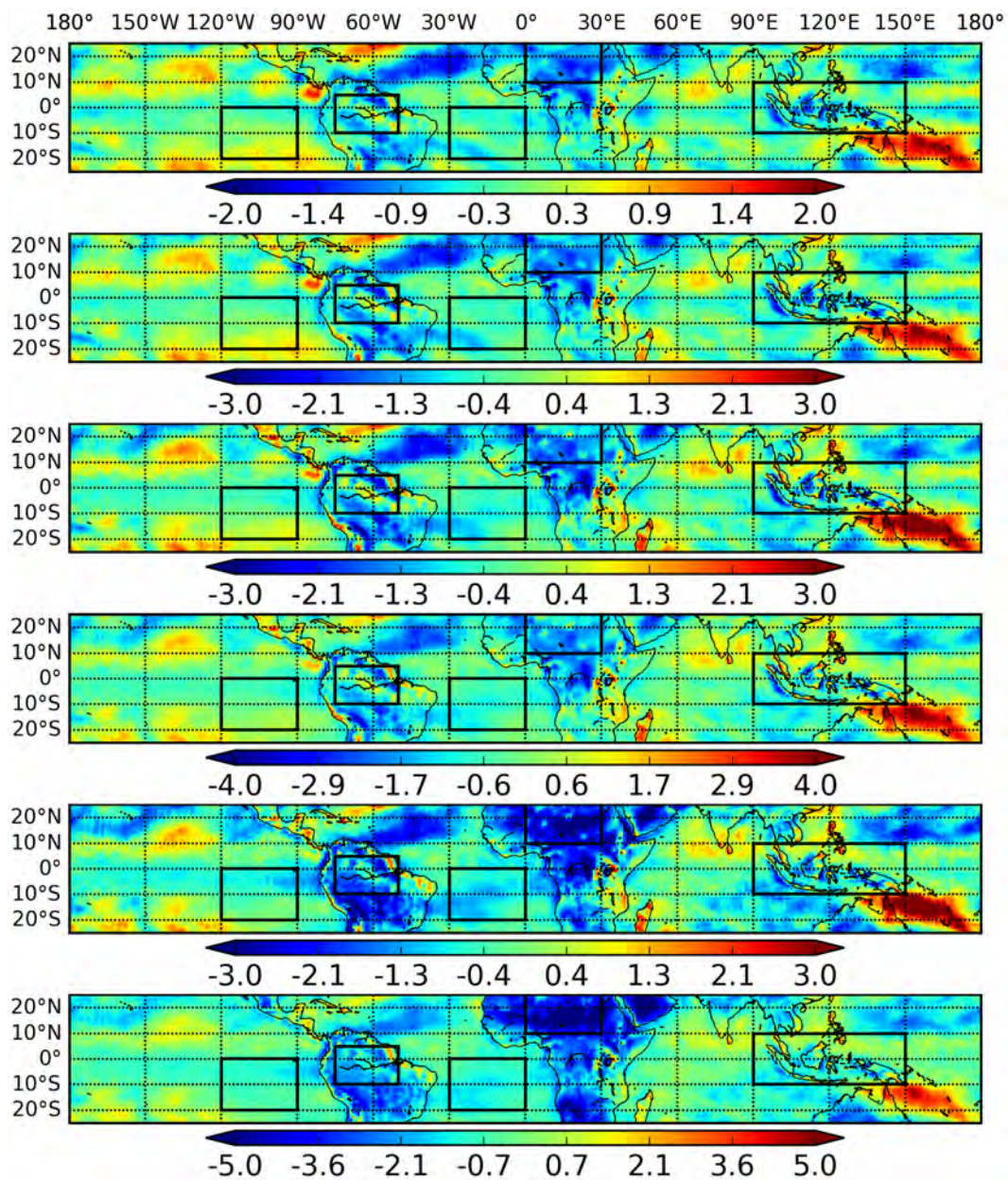


Figure 13. The coefficient b_1 (with respect to liquid) for the Fourier series fit. Plots from top to bottom are for SAPHIR channels 1-6, respectively.

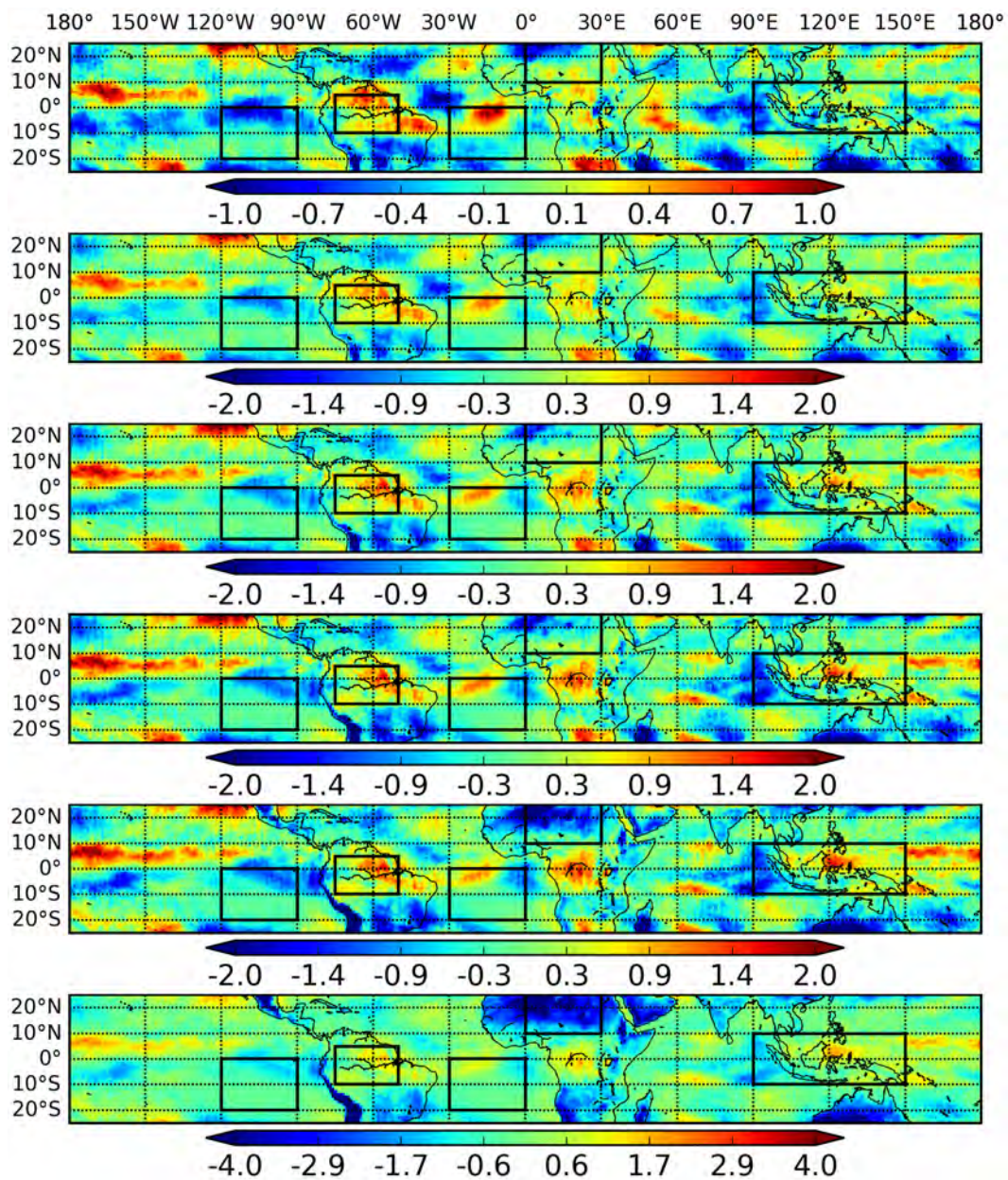


Figure 14. The coefficient a_2 (with respect to liquid) for the Fourier series fit. Plots from top to bottom are for SAPHIR channels 1-6, respectively.

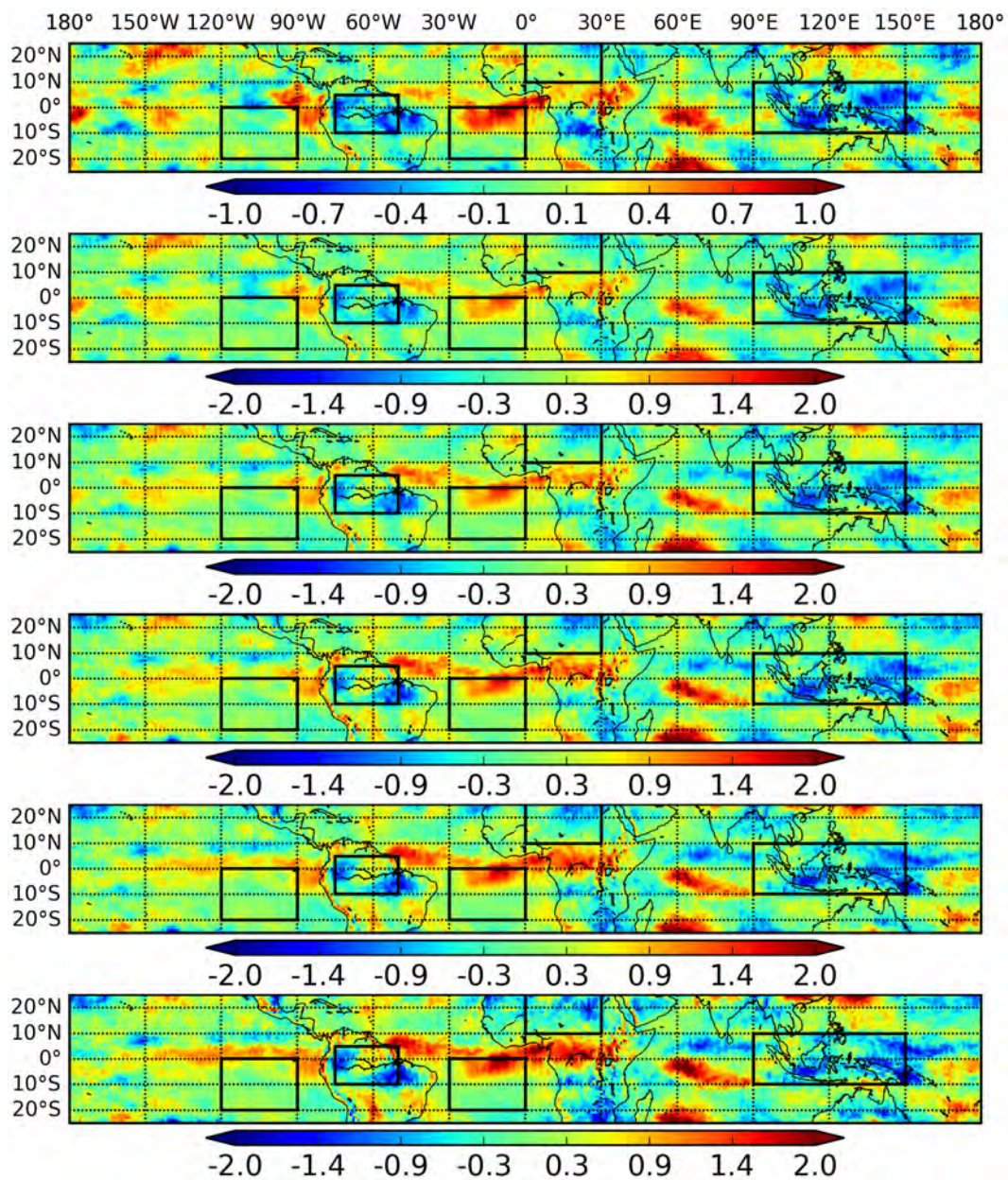


Figure 15. The coefficient b_2 (with respect to liquid) for the Fourier series fit. Plots from top to bottom are for SAPHIR channels 1-6, respectively.

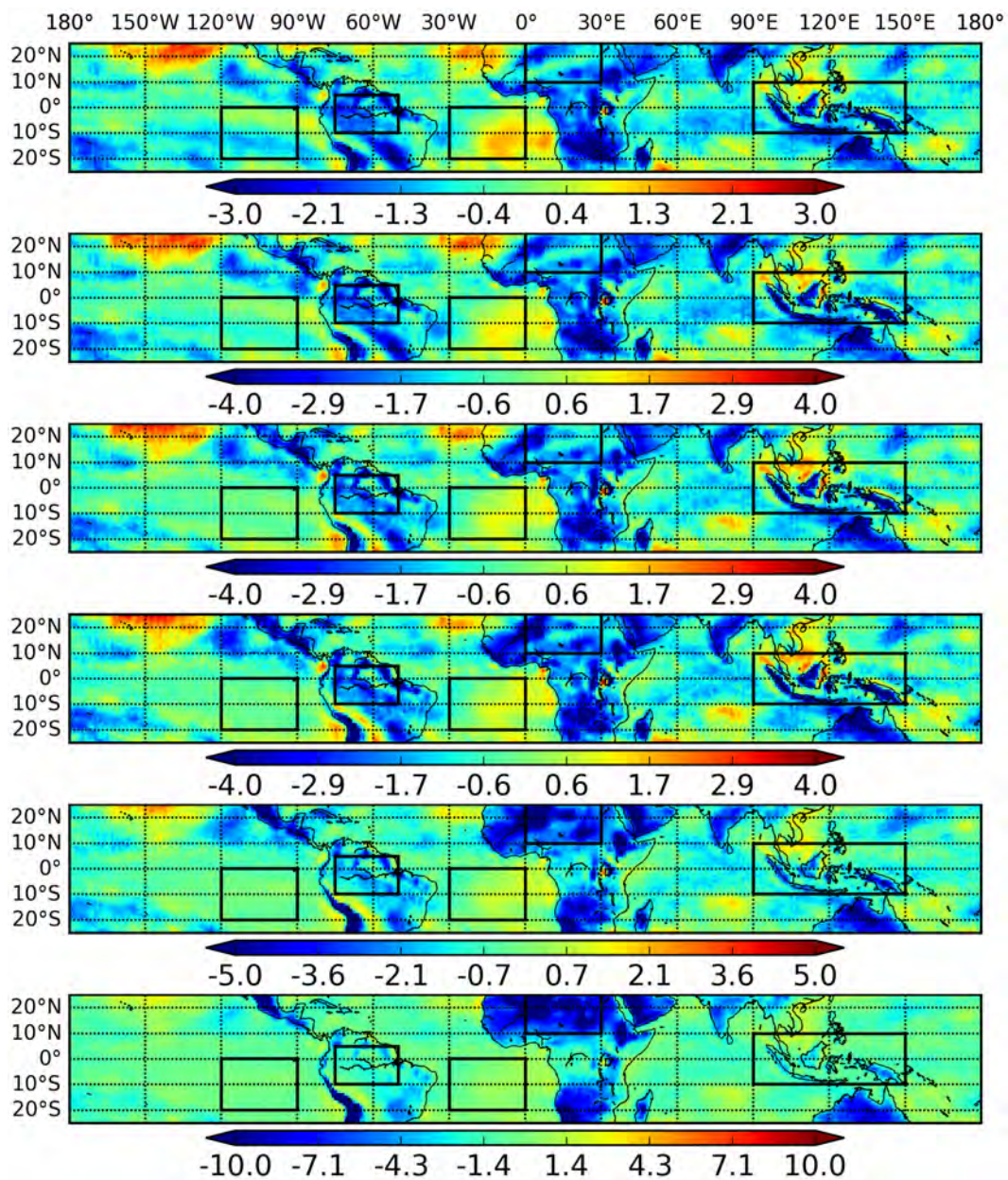


Figure 16. The coefficient a_1 (with respect to ice) for the Fourier series fit. Plots from top to bottom are for SAPHIR channels 1-6, respectively.

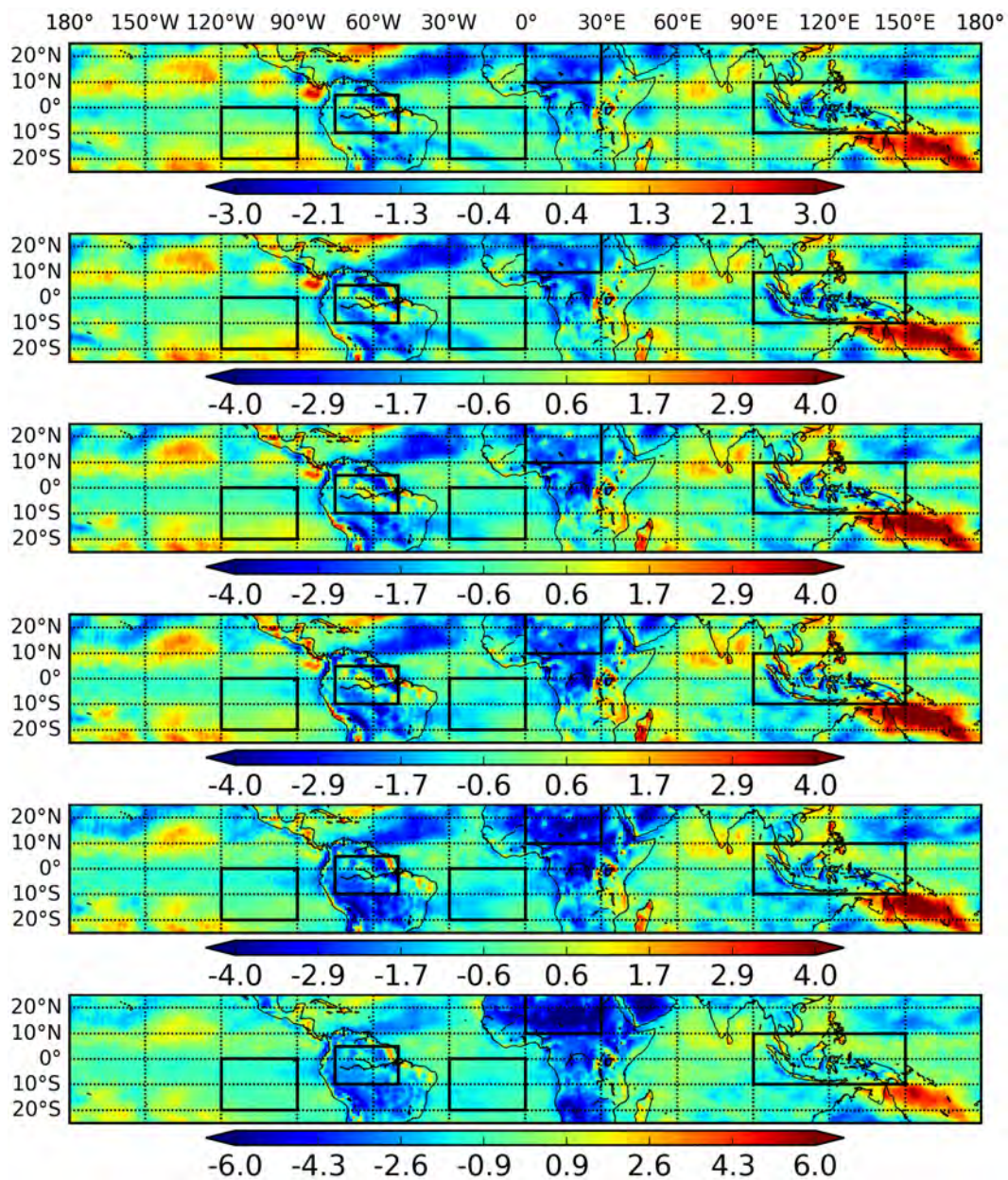


Figure 17. The coefficient b_1 (with respect to ice) for the Fourier series fit. Plots from top to bottom are for SAPHIR channels 1-6, respectively.

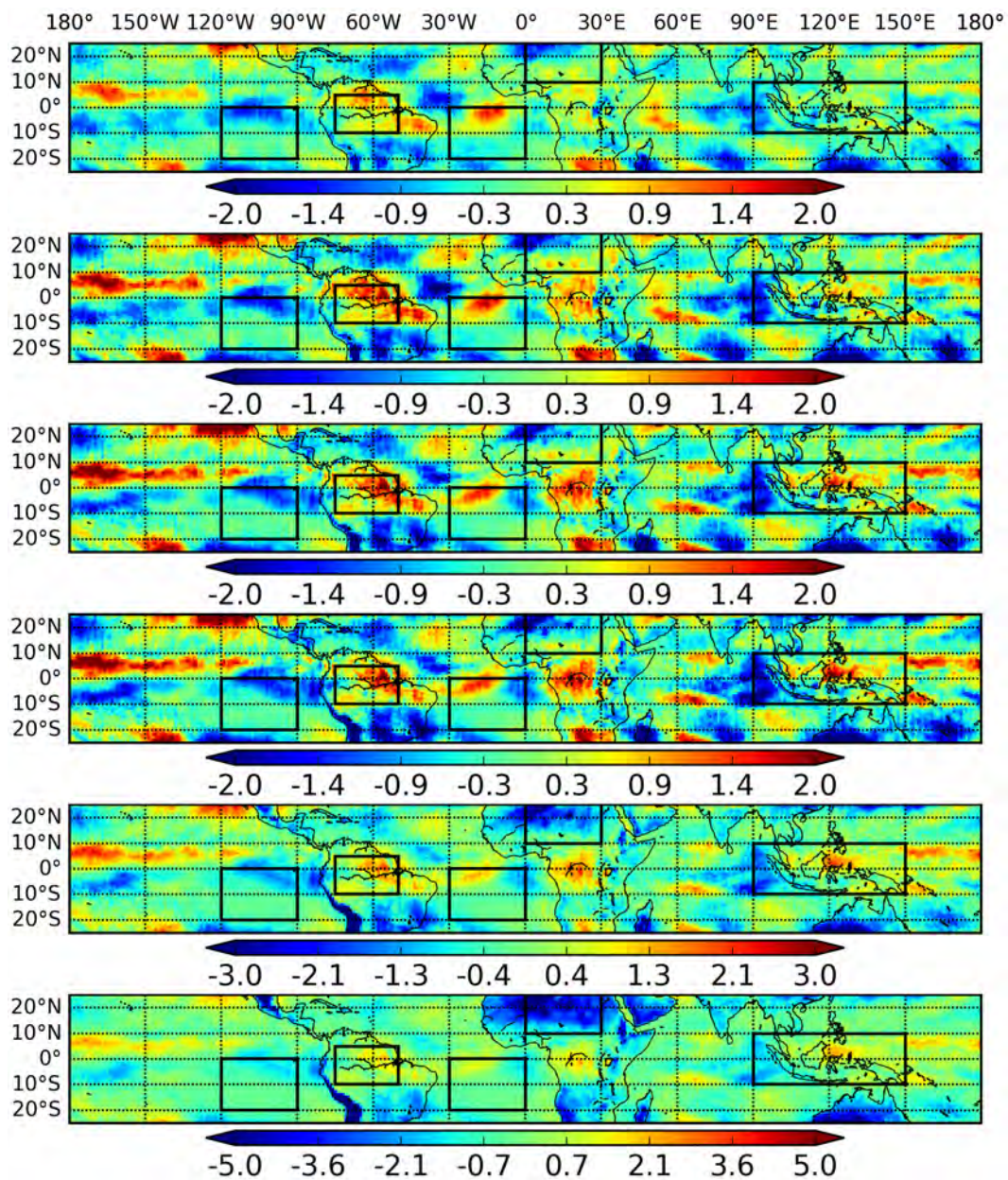


Figure 18. The coefficient b_2 (with respect to ice) for the Fourier series fit. Plots from top to bottom are for SAPHIR channels 1-6, respectively.

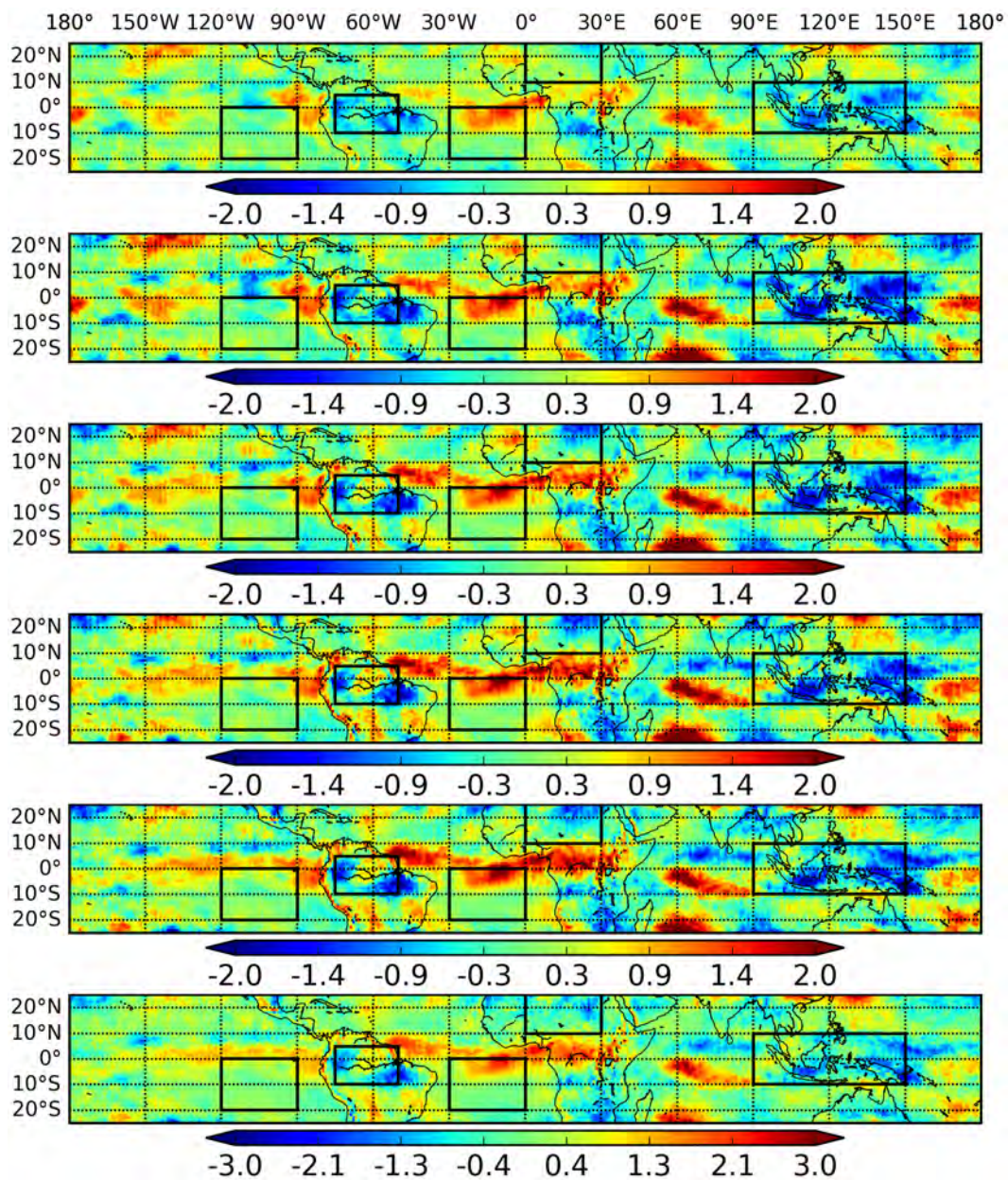


Figure 19. The coefficient b_2 (with respect to ice) for the Fourier series fit. Plots from top to bottom are for SAPHIR channels 1-6, respectively.

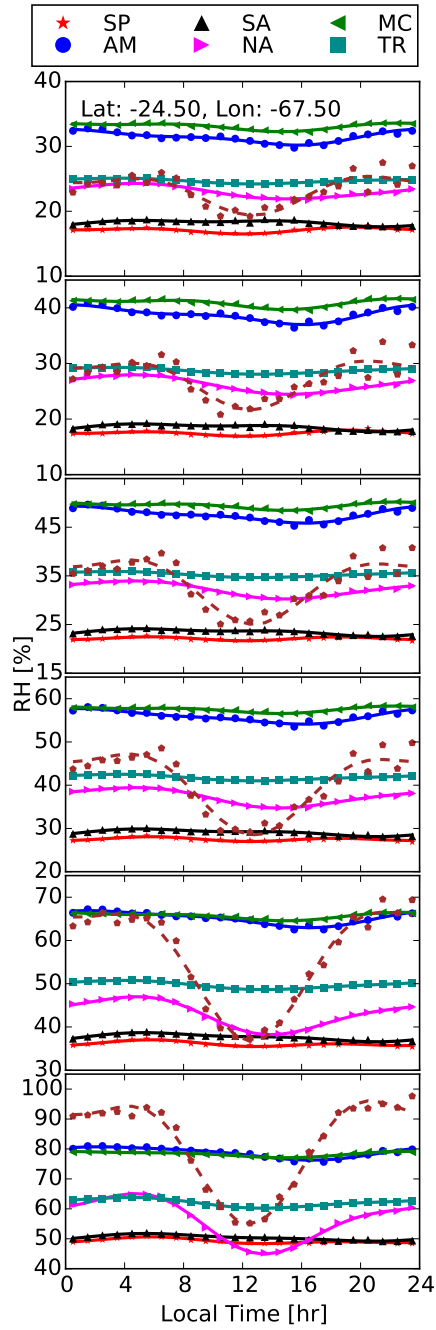


Figure 20. Diurnal cycle of layer-averaged RH_L as well as Fourier series fit for the selected regions. Plots from top to bottom are for SAPHIR channels 1-6, respectively.

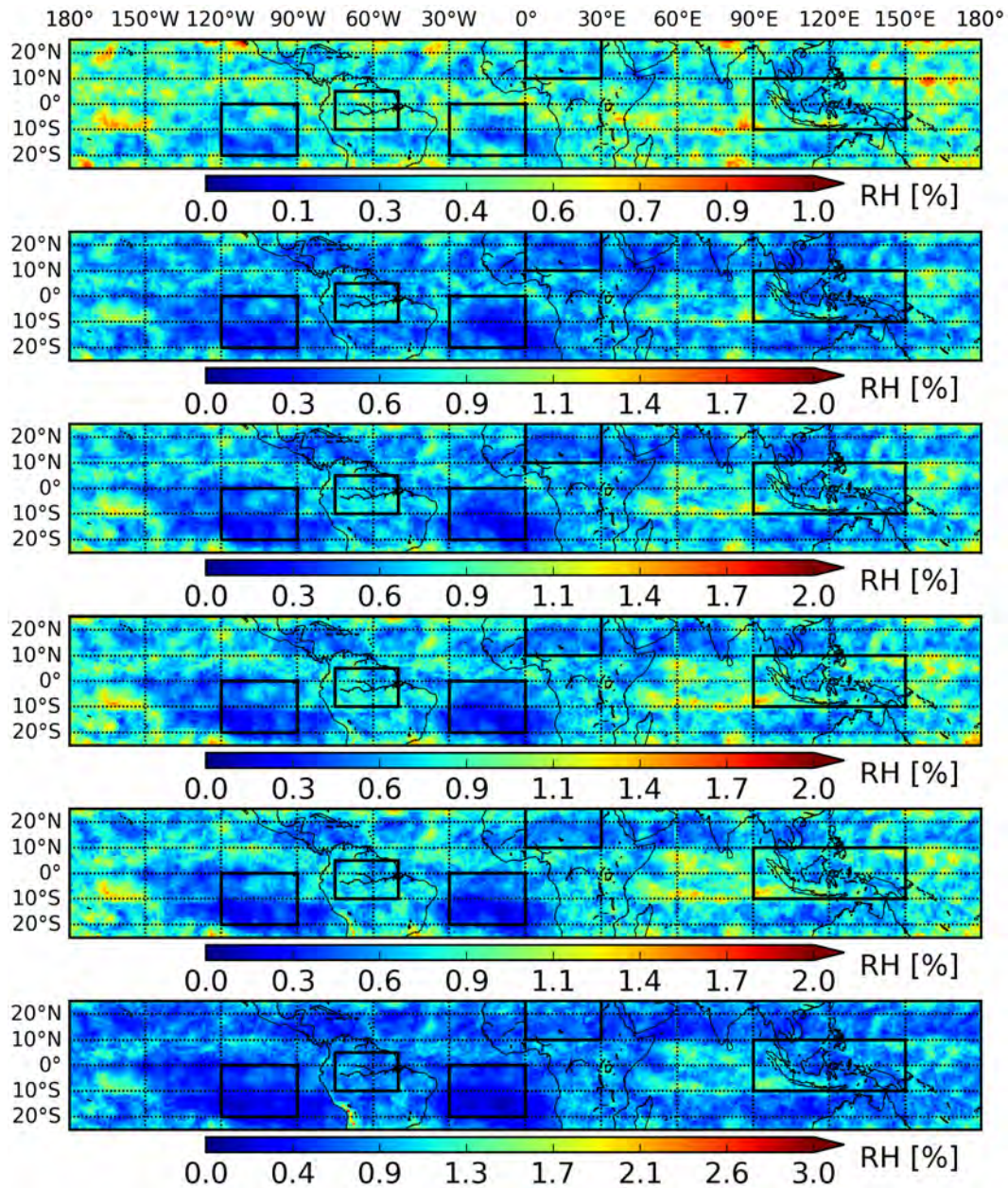


Figure 21. Mean absolute difference (with respect to liquid) between measurements and the fit for Fourier series. Plots from top to bottom are for SAPHIR channels 1-6, respectively.

5 Distribution Functions

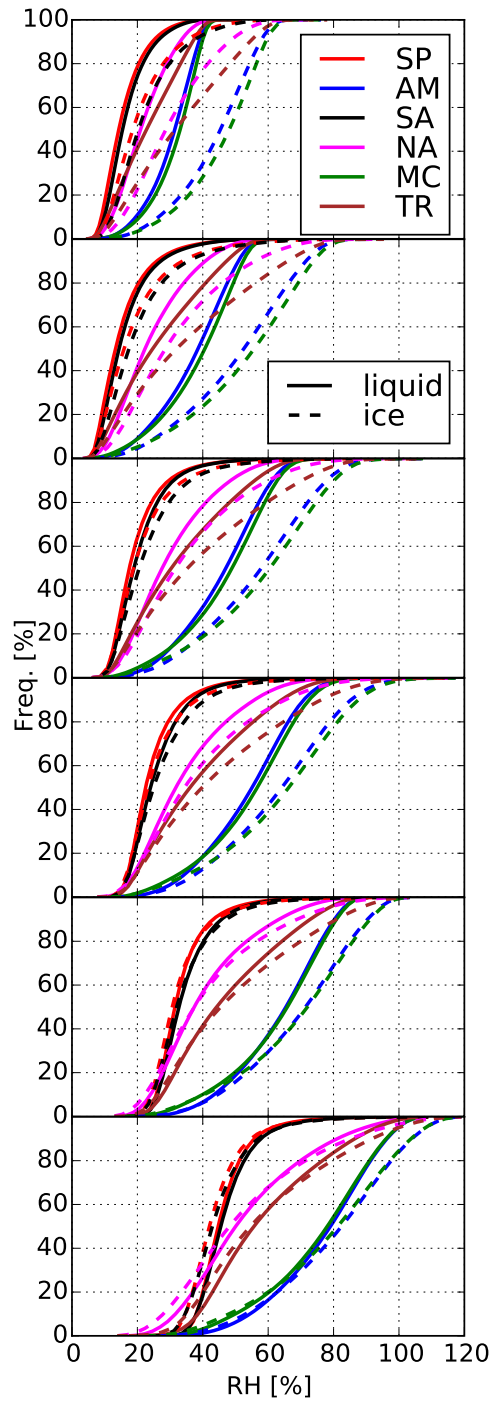


Figure 22. Cumulative probability distribution functions for relative humidity. Plots from top to bottom are for SAPHIR channels 1-6, respectively.